Shadowing effects in MIMO channels for personal area networks

Kåredal, Johan; Johansson, Anders J; Tufvesson, Fredrik; Molisch, Andreas

Published in:
[Host publication title missing]

DOI:
10.1109/VTCF.2006.47

2006

Shadowing Effects in MIMO Channels for Personal Area Networks

Johan Karedal[1], Anders J Johansson[1], Fredrik Tufvesson[1], and Andreas F. Molisch[1,2]
[1] Dept. of Electroscience, Lund University, Box 118, SE-221 00 Lund, Sweden.
[2] Mitsubishi Electric Research Labs, 201 Broadway, Cambridge, MA 02139, USA.
Email: {Johan.Karedal, Anders.J.Johansson, Fredrik.Tufvesson, Andreas.Molisch}@es.lth.se

***Abstract*— In this paper we analyze the effects of body shadowing in multiple-input-multiple-output (MIMO) channels used for personal area networks (PANs). We give physical reasoning to why PANs may experience two different types of shadowing, and to support our argument, we present results from a measurement campaign for three different PAN channels with human influence. The campaign is performed using different types of multi-element antenna devices; an access point, a body-worn device and two hand-held devices, conducted over a series of distances between 1-10 m. For each distance, a number of channel realizations are obtained by moving the antenna devices over a small area, and by rotating the persons holding the devices. The results show that it is suitable to distinguish between body shadowing (due to the rotation of the person holding the device) and shadowing due to surrounding objects (lateral movement). We also present a statistical model where the two types of shadowing are described as separate log-normal processes. Furthermore, we find that body shadowing has a big influence on the capacity of the investigated PAN channels.**

I. Introduction

In recent years there has been an increase of interest in wireless systems with high data rates but small coverage area. Such systems, commonly known as "personal area networks" (PANs), are often defined as a network where transmitter and receiver are separated no more than 10 m, and usually located within the same room. Due to the high required data rates, innovative transmission schemes have been proposed. Especially, MIMO (multiple-input−multiple-output) systems, i.e., systems with multiple antenna elements at both link ends, seem suitable [1], [2], [3].

MIMO systems promise high spectral efficiency and thus high data rates by allowing the transmission of multiple data streams without additional spectral resources [2], [3], [4]. For this reason, many theoretical as well as experimental investigations have been performed on different aspects of MIMO in the last 10 years [5]. It has been shown repeatedly that the wireless propagation channel has a key impact on both the information-theoretical limits and the performance of practical MIMO systems [6]. Correlation between the different antenna elements influences the eigenvalue distribution, and thereby the capacity. These effects have been first investigated for generic MIMO systems [2], [7], and were experimentally confirmed for MIMO-PANs in [8] and [9], which treat correlation properties and capacity issues for a base-station to hand-held terminal scenario.

Another important propagation effect is shadowing, i.e., variations of the received power due to obstruction of propagation paths by various objects. Shadowing has a very important impact on the capacity and bit error rate performance of MIMO systems. Commonly, shadowing is modeled as lognormally-distributed variations of the (distance-dependent, narrowband) pathloss; different values of the shadowing are obtained by moving the receiver over relatively large distances (on the order of one coherence length of the shadow fading) [10]. This model was originally devised for cellular systems, especially car-mounted receiver systems. It has been in widespread use and is also included in standardized models for cellular systems, like the 3GPP model [11], the COST 259 model [12], and the COST 273 model [13].

However, as we will show in this paper, this model is insufficient for many PANs: due to the body shadowing, variations occur not only by lateral movement, but also by rotation of the user, and/or movement of the antennas with respect to the body. It is thus preferable to distinguish between the shadowing caused by surrounding objects and the shadowing caused by the body. Different types of movements of the users lead to different types of shadowing, with different fading statistics and coherence times. This distinction between the two shadowing types is the main theme of the current paper. Our theory of "two types of shadowing" is tested and verified by a recent extensive MIMO measurement campaign for PAN applications.[1]

Thus, the key contributions of this papers are:

- We give physical reasoning that a PAN shows two types of shadowing, which have different importance depending on the type of movement.
- We support this argument with results from a recent measurement campaign.
- We compare the effects of the shadowing types at 2.6 and 5.2 GHz carrier frequency.
- We compare the results for several different scenarios performed with two hand-held devices, an access point and a body-worn device, each equipped with several antenna elements.

[1] In previous publications, we presented results for pathloss, correlation and delay properties in an access-point-to-PC scenario at 2.6 GHz [14], and results of the small-scale fading for a hand-held-to-hand-held scenario at 5.2 GHz [15]. In the former paper, we included a shadowing model, but since that was based on measurements *without* any significant variations of body shadowing, a "conventional" model was used.

1-4244-0063-5/06/$20.00 ©2006 IEEE

- We show how body shadowing affects the received power as well as the capacity of a MIMO system.
- We provide a statistical model for the two types of shadowing.

The remainder of the paper is organized the following way: Section II describes the different types of shadowing, and explains why different types of movement lead to different values of shadowing. Section III describes the setup for the measurements, and the physical environment in which the measurements were made. Section IV describes the measurement results, and Section V models those results. A summary and conclusions in Section VI wrap up this paper.

II. Shadowing Types

The well-known and standard way of describing the fluctuations in the received power of a wireless channel is as the combined effect of two fading processes: the small-scale fading and the large-scale fading, also known as shadowing [10]. The former is due to the constructive and destructive interference of the components impinging of the receiver, and is thus related to the relative $phases$ of the multipath components. The latter is due to changes in the average $power$ of the multipath components; it is typically assumed to be due to large-scale variations in the physical environment of the receiver. Variations of the shadowing thus occur when the mobile station moves (laterally) over large distances.

Traditionally, shadowing is described as a random process, with an amplitude probability density function that is log-normal (i.e., the shadowing attenuation expressed in dB is Gaussian), and an autocorrelation function that is exponential [16]. The correlation length is typically on the order of 10-100 m; in other words, the shadowing fluctuations at two points that are separated by one correlation length will be approximately decorrelated.

In PANs, however, a least one link end is typically controlled by a human being, as typical applications are wireless portable digital assistants (PDAs) or other hand held devices. Thus a strong human presence can be expected in the near field of at least one of the antenna devices, and hence one or several human bodies are likely to lead to shadowing. Human presence in a wireless channel, even with handheld devices, is not a new problem and has been studied for cellular networks for quite some time. However, the common method of including the human impact is as a time-invariant "bulk attenuation factor"; variations of the shadowing due to rotation by the user have to our knowledge not been modeled statistically. Furthermore, PANs also show an additional mechanism for shadowing variations as the relative position between the body and a hand-held device can change frequently.

We also note that the used device and antenna types affect the amount of shadowing inflicted by the human body, as the antenna patterns determine how much power will be received or transmitted through the body of the antenna device operator. Also, it is of importance where the antennas are mounted and how they are directed with respect to the body. Hence, the human body will, depending on the exact locations of Tx, Rx and human operator, add a different amount of shadowing on the received power. Thus, the assumption of the shadowing experienced by a receiver being constant for each Tx-Rx position is no longer valid, as if a person rotates, the amount of shadowing will change markedly. The total shadowing induced by the channel will thus be the sum of two parts, and hence it is reasonable to separate two types of shadowing: 1) the power variations due to the physical surroundings around Tx and Rx, and 2) the power variations due to the changes of body shadowing induced by the operator of the wireless device.

It is noteworthy that the two types of shadowing can have vastly different coherence lengths and times. In many cases, a user will not move laterally during the usage of e.g., a PDA. Thus the coherence time of the physical surroundings shadowing is infinite. However, during operation the user may often rotate and move the PDA with respect to the body, and thus coherence times for this type of shadowing can be on the order of seconds or less.

III. Measurement Setup

To verify the theories of the previous section, we use data from a recent measurement campaign performed using a number of possible PAN application antenna devices. This section briefly summarizes the measurement setup; for more details see [14].

The measurements were done with the RUSK LUND channel sounder that performs MIMO measurements based on the "switched array" principle [17]. Two frequency bands 2.6 ± 0.1 GHz and 5.2 ± 0.1 GHz were measured, each divided into 321 frequency points. The RUSK sounder allows to adjust the length of the test signal and the corresponding guard interval between two consecutive measurements. For our measurements a value of 1.6 μs was used for both. This corresponds to a resolvable "excess runlength" of multipath components of 480 m, which was more than enough to avoid overlap of consecutive impulse responses.

For PANs, especially for hand-held and body-worn devices, it is preferable to analyze the combined effect of channel, antennas, and human operators of the mobile station, using the same antenna configurations for the measurements that would also be used for the actual operation . For this reason, we concentrate on characterizing the "effective" channels that include the impact of antennas, structures on which the antennas are mounted (e.g., handheld devices) and human bodies.

A. Measurement Scenarios

In order to capture different amounts of body shadowing, three different scenarios were measured: (i) from an access point (AP) to a body-worn device (BW), (ii) from an AP to a hand-held device (HH) and (iii) from a HH to another HH. Different antenna devices were used to perform measurements for different scenarios. All antenna devices were equipped with several (in some cases dual-polarized; DP) antenna elements, as can be seen in Fig. 1. The number of elements and antenna types used for each antenna device are described in Table I, where the number of elements (in

TABLE I

ANTENNA TYPES USED IN THE DIFFERENT DEVICES

	2.6 GHz		5.2 GHz	
	Type	Elements	Type	Elements
AP	DP patch	$2 \times 8 \times 2$	DP patch	$2 \times 2 \times 2$
HH (Tx)	patch	2	slot	4
HH (Rx)	PIFA	4	slot	4
BW	N/A	N/A	DP patch	$2 \times 1 \times 2$

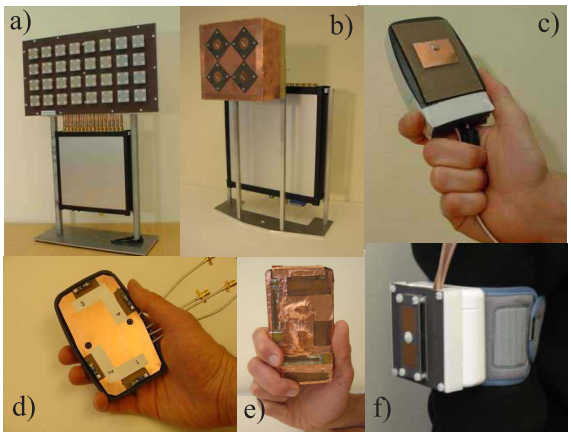

Fig. 1. The antenna devices used in the different scenarios: a) AP 2.6 GHz (middle rows used), b) AP 5.2 GHz, c) HH (Tx) 2.6 GHz, d) HH (Rx) 2.6 Hz, e) HH (Tx and Rx) 5.2 GHz, f) BW 5.2 GHz.

applicable cases) are given as (number of element rows) $\times$ (number of element columns) $\times$ (number of polarization).

In the HH-to-HH scenario, Tx and Rx were held in the right hand of two standing persons (referred to as *device holders*). To capture the effects of body shadowing, nine measurements with different directions (referred to as *orientation* $1-9$) of the device holders (and hence, the devices) were made at each Tx-Rx position (see Fig. 2). Additionally, during each measurement the Tx device was slowly moved over a small area (30 cm $\times$ 30 cm) allowing the channel sounder to sample 10 different snapshots of the channel with small spatial offsets.

In the AP-to-HH scenario, the AP was used as Tx. The antenna device was mounted on a tripod and elevated to ceiling height (2.2 m) in order to resemble a true access point. The HH device was held in the right hand of the device holder, as in the HH-to-HH scenario. Rx positions were selected as typical working positions, i.e., with the device holder sitting at a desk. Similar to the HH-to-HH scenario, four measurements with different orientations of the Rx device holder were made at each Rx position, along with the sampling of 10 snapshots during a slow movement of the Rx device.

The AP-to-BW scenario is similar to the AP-to-HH scenario in the sense that the same Tx (AP) setup, Rx positions as well as number of orientations and snapshots were used. However, in this scenario, the Rx device holder carried the BW device on the right arm (biceps). This scenario was only measured for the 5.2 GHz frequency band.

B. Measurement Environment

The measurements were conducted in an office environment of the E-building at Lund University, Sweden. The offices are located in a modern building, made of brick and reinforced concrete, where adjacent offices are separated by gypsum wallboards.

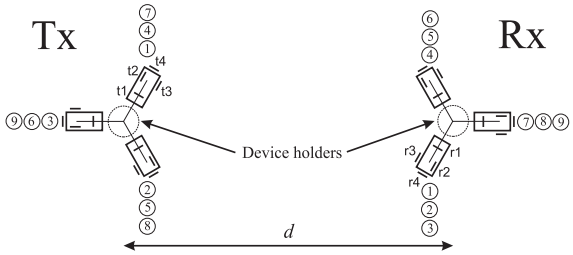

Fig. 2. The nine possible antenna orientations at each Tx-Rx separation d in the HH-to-HH scenario. Circled numbers show how Tx and Rx were oriented during each measurement; t1, r1, t2, etc. show the antenna elements of each HH device.

IV. MEASUREMENT RESULTS

A. Shadowing by Body and Surrounding Objects

To investigate the influence of rotations and body shadowing, we determine the total received power for two cases:

1) Average received power for each snapshot and rotation, i.e., for a Tx-Rx separation d, the received power $P_1(d, s_i, o_i)$ for snapshot s_i and orientation o_i is determined as the average over antennas and frequency.
2) Average received power for each Tx-Rx separation, i.e., for a Tx-Rx separation d, the received power $P_2(d)$ is determined as the average over antennas, frequency, snapshots and orientation.

Fig. 3 shows a scatter plot of $P_1(d, s_i, o_i)$ and $P_2(d)$ for the HH-to-HH scenario for the 5.2 GHz band. For this scenario, the distance dependence of the pathloss is very weak; the estimated pathloss exponent is only 0.3. However, in this, as well as in other scenarios where the pathloss exponent is larger, we note that $P_2(d)$ varies around the distance dependent decay, whereas $P_1(d, s_i, o_i)$ varies around $P_2(d)$. In other words, the variations for a given rotation *and* distance are much smaller than the variations for a given distance (using all orientations in the ensemble over which the variation is determined). The results thus confirm our theories of Section II, and hence we find it suitable to divide the shadowing into two parts, one caused by the rotation of the device holder (i.e., the variations of $P_1(d, s_i, o_i)$ around $P_2(d)$), and one caused by the physical surroundings at each Rx position (the variations of $P_2(d)$).

Fig. 4 again shows the received power of the 5.2 GHz HH-to-HH scenario, where in contrast to Fig. 3, averaging has been done over the snapshots, but *not* the orientation. Comparing measurements where at least one antenna device is shadowed by the device holder (marked as circles in Fig. 3) with measurements without body shadowing (marked as triangles), it can be seen that the magnitude of the body shadowing is in the range of 10 dB.

B. Correlation of Shadowing

To evaluate whether the shadowing experienced by different antenna elements at the receiving antenna device, is similar or

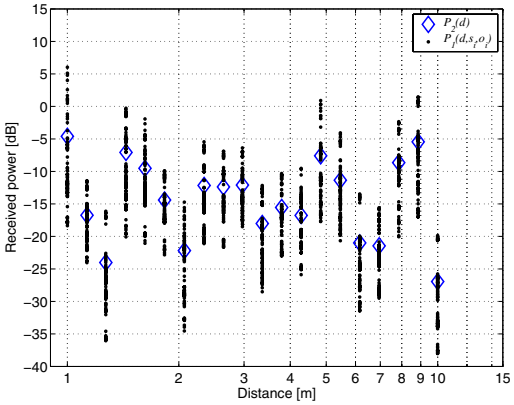

Fig. 3. Received power for the measurements of the 5.2 GHz HH-to-HH scenario. The dots represent P_1 whereas diamonds represent P_2.

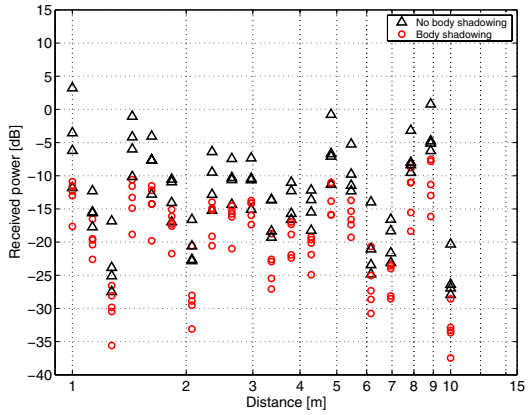

Fig. 4. Received power for the measurements of the 5.2 GHz HH-to-HH scenario. In this figure, the power has been averaged over the snapshots to visualize the magnitude of the body shadowing. Triangle markers are measurements without (significant) body shadowing, i.e., orientations 1, 2, 4 and 5, whereas circle markers are measurements with at least one antenna device shadowed by a device holder, i.e., orientations 3, 6, 7, 8, and 9.

not, we derive the correlation between the small-scale averaged (over the 321 frequency subchannels) power received in each Rx element during the 10 channel samples as described by Sec. III-A. With measured rms delay spread values in the range of 10 ns (for all scenarios), and hence a 0.9 coherence bandwidth of roughly 20 MHz, our measured bandwidth of 200 MHz ensures enough frequency samples to average out the small-scale fading. We thus determine the correlation coefficient between the received power at receive elements i and j as

$$r_{ij} = \frac{E\left[P_{i|\text{ssa}} P_{j|\text{ssa}}\right] - E\left[P_{i|\text{ssa}}\right] E\left[P_{j|\text{ssa}}\right]}{\sigma_{P_{i|\text{ssa}}} \sigma_{P_{j|\text{ssa}}}}$$

where $P_{i|\text{ssa}}$ is the small-scale averaged power samples received at element i during the 10 snapshots, $\sigma_{P_{i|\text{ssa}}}$ and $E\{\sim\}$ is the expectation operation (over the snapshots).

The results show that the shadowing correlation is fairly low, with correlation coefficients in the magnitude of $0.3 - 0.4$ for nearly all scenarios, irrespective of whether the measurements are LOS or not, and what frequency band is considered. The

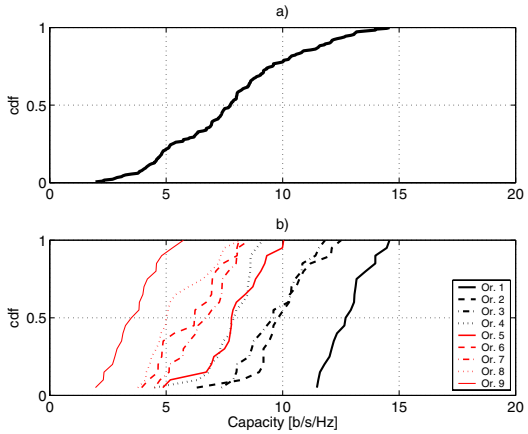

Fig. 5. Capacity cdf:s for the 5.2 GHz HH-to-HH measurements; a) includes *all* measurements (and hence both shadowing types) whereas in b) the nine cdf:s ("Or. 1-9") correpond to each measured device orientation (hence, for each one, only shadowing due the physical environment is included).

AP-to-BW scenario shows the highest correlation, especially if co-polarized and cross-polarized channels are separated (this is possible since the polarization directions are well maintained throughout the measurements). This result is reasonable since all the BW antennas essentially "see" the same environment (in contrast to the HH devices). However, the correlation coefficient is still only as high as 0.45 for co-polarized LOS channels (0.35 for cross-polarized).

C. Impact of Shadowing on Capacity

We calculate the capacity for 4×4 MIMO systems (for an SNR of 10 dB), when normalizing to the same Tx power for all orientations (corresponding to a power limited case).[2] The variations in mean capacity are shown in Fig. 5, where the mean has been taken over the small-scale fading, i.e., over frequency subchannels and snapshots (See Sec. III-A). In Fig. 5a, measured capacity for all orientations are used for the cdf, and hence both types of shadowing are included. In Fig. 5b on the other hand, each cdf corresponds to a particular measured orientation (see Fig. 2) and thus each cdf only includes the shadowing due to the physical surroundings. We conclude that the variations in capacity depend highly on whether both shadowing types are included or not.

V. Statistical Model

Based upon the results and the discussion of the previous section, we find it suitable to model the received power (in dB) for a given Tx-Rx separation distance as

$$P(d) = P(d_0) - 10n \log_{10}\left(\frac{d}{d_0}\right) + S_{\text{sur}} + S_{\text{body}}$$

where difference from the classical pathloss model [10] is that there are *two* added random variables S_{sur} and S_{body}. The former represents the shadowing effects caused by the physical environment of the antenna device(s), whereas the latter represents the shadowing effects induced by the body

[2]Note that this removes the influence of the distance dependent pathloss.

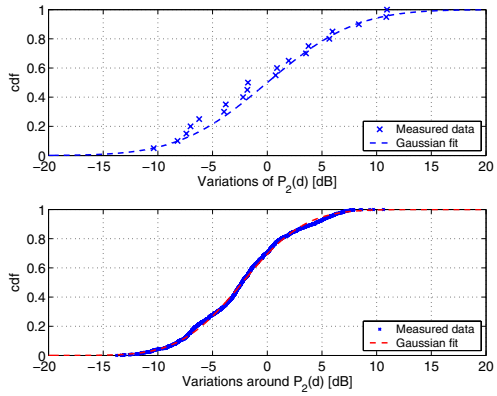

Fig. 6. Variations of $P_2\,(d)$ (top) and variations of $P_1\,(d, s_i, o_i)$ around $P_2\,(d)$ (bottom) for the HH to HH scenario, 5.2 GHz.

TABLE II

SHADOWING PARAMETERS

		2.6 GHz			5.2 GHz		
		$\sigma_{S_{\text{body}}}$ [dB]	$\sigma_{S_{\text{sur}}}$ [dB]	n	$\sigma_{S_{\text{body}}}$ [dB]	$\sigma_{S_{\text{sur}}}$ [dB]	n
LOS:	AP-HH	2.3	2.3	1.31	2.1	2.7	1.24
	AP-BW	–	–	–	4.4	2.7	0.06
	HH-HH	4.2	4.2	2.65	4.5	6.4	0.32
NLOS:	AP-HH	2.2	5.1	2.04	2.0	4.7	1.80
	AP-BW	–	–	–	4.2	4.2	2.55
	HH-HH	3.6	3.6	2.24	3.6	2.7	2.75

and orientation of the operator of the wireless device. From the measurements (cf. Fig. 3), S_{sur} and S_{body} are found to be well described by lognormal distributions. Hence, let $S_{\text{sur}}|_{\text{dB}} \sim N\left(0, \sigma^2_{S_{\text{sur}}}\right)$ and $S_{\text{body}}|_{\text{dB}} \sim N\left(0, \sigma^2_{S_{\text{body}}}\right)$. Note that this model implies that *one* value for S_{sur} is associated with every measurement location. Model parameters are given in Table II.

Comparing shadowing parameters from the different scenarios, we note that the effects of the body shadowing are comparable with those of the shadowing due to the physical environment. The HH-to-HH scenarios exhibit larger power variations due to body shadowing than the AP-to-HH scenarios, which is reasonable, since the former includes rotating the antenna devices at both link ends. The higher standard deviation of the body shadowing in the AP-to-BW scenario, compared to the AP-to-HH scenario, is most likely explained by the design of the antenna devices. Whereas the elements of the HHs are pointing in different directions, all elements of the BW are pointing in one and the same. Hence, the BW will be more sensitive to rotations than the HH.

It is also notable that the results are very consistent over frequency; there is hardly any difference in shadowing standard deviation between the two measured frequency bands. The only major difference is that of the pathloss exponent for the HH-to-HH LOS scenario; the 2.6 GHz measurements show a much heavier distance dependence than the 5.2 GHz measurements.

VI. SUMMARY AND CONCLUSIONS

We have presented an analysis of shadowing effects in MIMO systems for typical PAN applications. We find it suitable to distinguish between two types of shadowing; (i) body shadowing (due to the rotation of the device holder) and (ii) shadowing due to the physical environment (lateral movement). Based upon the results we have derived a statistical model describing the two shadowing types. Additionally, we have shown how the two types of shadowing can have a big impact on capacity.

ACKNOWLEDGEMENTS

We thank Bristol University, and especially Prof. Mark Beach, for letting us perform measurements with their antennas. Part of this work was funded by the MAGNET project (contract no. 507102) of the European Union, an INGVAR grant of the Swedish Foundation for Strategic Research, and a grant from the Swedish Science Council.

REFERENCES

[1] J. H. Winters, "On the capacity of radio communications systems with diversity in Rayleigh fading environments," *IEEE Journal on Selected Areas in Communications*, vol. 5, pp. 871–878, June 1987.

[2] G. J. Foschini and M. J. Gans, "On limits of wireless communications in a fading environment when using multiple antennas," *Wireless Personal Communications*, vol. 6, pp. 311–335, Feb. 1998.

[3] A. Paulraj, D. Gore, and R. Nabar, *Multiple Antenna Systems*. Cambridge, U.K.: Cambridge University Press, 2003.

[4] I. E. Telatar, "Capacity of multi-antenna Gaussian channels," *European Transactions on Telecommunications*, vol. 10, Nov.-Dec. 1999.

[5] D. Gesbert, M. Shafi, D.-S. Shiu, P. J. Smith, , and A. Naguib, "From theory to practice: An overview of MIMO space-time coded wireless systems," *IEEE J. Selected Ares Comm.*, vol. 21, pp. 281–302, 2003.

[6] A. F. Molisch and F. Tufvesson, "MIMO channel capacity and measurements," in *Smart Antennas - State of the art* (T. Kaiser, ed.), Eurasip publishing, 2005.

[7] C.-N. Chuah, D. N. C. Tse, J. M. Kahn, and R. A. Valenzuela, "Capacity scaling in MIMO wireless systems under correlated fading," *IEEE Trans. on Information Theory*, vol. 48, no. 3, pp. 637–650, 2002.

[8] W. A. T. Kotterman, G. F. Pedersen, K. Olesen, and P. Eggers, "Correlation properties for radio channels from multiple base stations to two antennas on a small handheld terminal," in *Proc. IEEE Vehicular Technology Conference 2002 fall*, vol. 1, pp. 462–466, 2002.

[9] W. A. T. Kotterman, G. F. Pedersen, and K. Olesen, "Capacity of the mobile mimo channel for a small wireless handset and user influence," in *Proc. The 13th IEEE International Symposium on Personal, Indoor and Mobile Radio Communications*, vol. 4, pp. 1937–1941, 2002.

[10] A. F. Molisch, *Wireless Communications*. Chichester, West Sussex, UK: IEEE Press–Wiley, 2005.

[11] G. Calcev, D. Chizhik, B. Goeransson, S. Howard, H. Huang, A. Kogiantis, A. F. Molisch, A. L. Moustakas, D. Reed, and H. Xu, "A wideband spatial channel model for system-wide simulations," *IEEE Transactions on Vehicular Technology*, 2006. in press.

[12] M. Steinbauer and A. F. Molisch, "Directional channel models," in *Flexible Personalized Wireless Communications* (L. Correia, ed.), ch. 3.2, pp. 135–144, Wiley, 2001.

[13] A. F. Molisch and H. Hofstetter, "The COST273 MIMO channel model," in *COST273 final report* (L. Correia, ed.), Springer. to appear in 2006.

[14] A. Johansson, J. Karedal, F. Tufvesson, and A. F. Molisch, "MIMO channels measurements for personal area networks," in *Proc. IEEE Vehicular Technology Conference 2005 spring*, 2005.

[15] J. Karedal, A. J. Johansson, F. Tufvesson, and A. F. Molisch, "Characterization of MIMO channels for handheld devices in personal area networks," in *Proc. European Signal Processing Conference 2006*.

[16] M. Gudmundsson, "Correlation model for shadow fading in mobile radio systems," *IEEE Electronics Letters*, vol. 27, pp. 2145–2146, Nov. 1991.

[17] R. Thomae, D. Hampicke, A. Richter, G. Sommerkorn, A. Schneider, U. Trautwein, and W. Wirnitzer, "Identification of the time-variant directional mobile radio channels," *IEEE Trans. on Instrumentation and measurement*, vol. 49, pp. 357–364, 2000.